J Mater Sci (2010) 45:4994–5001
DOI 10.1007/s10853-010-4364-0

ICAM 2009

# Physicochemical and structural characteristics of TiC and VC thin films deposited by DC reactive magnetron sputtering

**C. Aguzzoli · C. A. Figueroa · G. V. Soares · I. J. R. Baumvol**

Received: 25 November 2009 / Accepted: 27 February 2010 / Published online: 12 March 2010


**Abstract** Vanadium carbide and titanium carbide films were deposited on Si substrates by direct current reactive magnetron sputtering, varying the substrate temperature during deposition and the reactive gas ($CH_4$) pressure. The physicochemical and structural properties of the films were characterized for stoichiometric films (V/C = 1 and Ti/C = 1), which display good performance concerning wear, friction, and corrosion. The techniques used to characterize the films were Rutherford backscattering spectrometry in channeling geometry, $^{12}C(\alpha,\alpha)^{12}C$ nuclear resonant scattering, glancing angle X-ray diffraction, X-ray reflectometry, and X-ray photoelectron spectroscopy. The results revealed that the ideal conditions for deposition of these films are a $CH_4$ partial pressure of $0.5 \times 10^{-3}$ mbar and a substrate temperature of 400 °C. In such conditions, the deposition rates are 7 nm $s^{-1}$ for TiC and 8.5 nm $s^{-1}$ for VC at a target power density of 5.5 W $cm^{-2}$. The density of the films, as determined here by X-ray reflectometry, are slightly higher than those for the bulk materials.

## Introduction

Transition metals carbides such as TiC, TaC, VC, and others are widely used as protective coatings owing to their high hardness and wear resistance, high thermal and chemical stability, as well as biocompatibility [1–7]. However, TiC has a poor oxidation resistance at high temperatures [8, 9]. These applications may involve very severe working conditions, like in machining, cutting, and drilling, in which near-surface temperatures may be as high as 750 °C.

The excellent performance against wear of TiC and VC protective coatings can be foreseen from the hardness ($H$) to Young modulus ($E$) ratios, a parameter commonly used to evaluate the wear resistance of the coatings [10, 11]. This is the so called elastic strain to failure, which has been proposed and consistently used [12, 13] to evaluate the resistance to plastic deformation of thin film coatings and to predict their resistance to wear. Thus, a high $H^3/E^2$ ratio indicates a high resistance of the coating to plastic deformation and, presumably, a high wear resistance as well, besides low stiffness. TiC does indeed display very attractive $H^3/E^2$ figures. The frictional properties of these materials are also superior, owing to the extremely fine grain dispersion of the thin film coatings [1].

There are many routes to deposit these hard coatings, like chemical vapor deposition (CVD) [14], pulsed laser deposition (PLD) [15], and physical vapor deposition (PVD) [16]. The advantage of PLD and PVD is that with these techniques we can deposit compound films at lower substrate temperatures [17, 18]. This is especially convenient in order to preserve the bulk properties of steel engineering components as obtained by thermal annealing.

Other aspects are also important for the final performance of the coatings [7]. One of them is the crystallinity of the hard coatings, which is directly correlated to the substrate temperature during deposition [19]: The higher the substrate temperature, the higher the crystalline order of the coating. It was also observed that if the content of the reactive gas changes, the crystallinity changes too [20]. In the case of vanadium carbide (VC), it was seen that the partial pressure of the reactive gas ($CH_4$) in the gas mixture

C. Aguzzoli (✉) · I. J. R. Baumvol
Universidade Federal do Rio Grande do Sul, Porto Alegre, RS, Brazil
e-mail: caguzzol@ucs.br

C. Aguzzoli · C. A. Figueroa · G. V. Soares · I. J. R. Baumvol
Universidade de Caxias do Sul, Caxias do Sul, RS, Brazil

that supports the plasma has a significant influence on the crystalline structure [19]. In titanium carbide (TiC) films, the partial pressure of the reactive gas, either methane or acetylene, has a strong influence on crystalline phase formation [20, 21] as well as on the hardness of the coatings. Furthermore, the C excess in TiC films was seen to decrease the film hardness [20].

In the present work, we investigate the elementary composition and the physicochemical and structural properties of TiC and VC films deposited by direct current (DC) reactive magnetron sputtering. Different contents of $CH_4$ and different substrate temperatures during deposition were accessed in order to investigate the influence of these deposition parameters on the physicochemical and structural characteristics of the films.

## Experimental

TiC and VC thin films were deposited on single-crystalline silicon(001) wafers by DC reactive magnetron sputtering, using a Ar/$CH_4$ gas mixture. Table 1 gives typical deposition parameters that led to the deposition of stoichiometric TiC and VC films, as described below.

The elementary composition of the films was determined by Rutherford backscattering spectrometry (RBS) [22] using $He^+$ ions incident at 2 MeV. This method allows also the determination of film thickness, using the density of the films obtained from XRR measurements. The areal densities of Ti, V, and C were determined using standards of Bi-implanted Si and C-implanted Si. Since the small C signal in the RBS spectra overlaps the intense Si substrate signal, rendering it difficult to quantify C, the channeled-RBS technique [23] was used here, where the <001> axis of the Si substrate was aligned with the direction of incidence of the $He^+$ beam, detecting the backscattered particles at 165° with the direction of incidence of the beam. Although in channeling geometry the Si-background contribution to the RBS spectra has been considerably reduced, the quantification of C in the films still bares an experimental error significantly larger than that for Ti and V.

**Table 1** Deposition parameters of thin films deposited by DC reactive magnetron sputtering

| | TiC and VC | |
|---|---|---|
| Base pressure (mbar) | $8.0 \times 10^{-7}$ | |
| Ar partial pressure (mbar) | $3 \times 10^{-3}$ | |
| $CH_4$ partial pressure (mbar) | $0.5 \times 10^{-3}$ | |
| Source-to-substrate distance (cm) | 12 | |
| Target power density (W $cm^{-2}$) | 2.7 | 5.5 |
| Deposition rate (nm $min^{-1}$) | 3.3 | 7 |

In order to reduce the experimental error in C quantification, the $^{12}C(\alpha,\alpha)^{12}C$ resonant scattering at 4.26 MeV [24–26] was used, taking advantage of the much higher cross section of this resonance, which is also narrow enough in energy to allow for C profiling [24–26] in the films. This method increases the C signal-to-noise ratio by at least a factor of 10 as compared to RBS, thus improving significantly the accuracy of the C quantification. A SiC (0001) single-crystalline wafer was used here as a standard for C quantification.

Glancing angle X-ray diffraction (GAXRD) and X-ray reflectometry (XRR) analyses were performed using a Shimadzu XRD-6000 apparatus, with Cu K$\alpha$ radiation ($\lambda = 1.54$ Å) at an incidence angle of 2°, in order to determine the crystalline structure of the films and density, respectively.

Chemical analysis was accomplished by X-ray photoelectron spectroscopy (XPS). An *Omicron Multiprobe Sphera* instrument was used, with a Mg K$\alpha$ (1256.3 eV) X-ray source. The energy resolution of the spectrometer was 0.9 eV.

## Results and discussion

### Composition

Typical RBS spectra in channeling geometry for 2 MeV incident $He^+$ ions from TiC and VC samples are shown in Fig. 1. The insets show the C signal energy regions, after subtraction of the Si-background contribution. One can verify from these spectra that the concentration of impurities in the films, for example O, Fe, Cr, and others are all below the sensitivity limit of RBS, namely below $10^{14}$ at. $cm^{-2}$ (about 1/10 of a monolayer). The presence of impurities would affect significantly the hardness and the adhesion of the coatings to the substrate.

Figure 2a, b shows typical $^{12}C(\alpha,\alpha)^{12}C$ resonant scattering spectra at increasing energies of the incident $He^+$ ions, for a TiC/Si and VC/Si thin film samples, starting at an energy value below the resonance energy of 4.26 MeV. At the resonance energy, the C peak in the spectrum is associated to the C contamination layer at the sample surface [24–26]. For progressively larger energies than the resonance energy, the C peak area in the spectrum is directly proportional to the C concentration at increasingly larger depths [24–26], such that a C profile can be extracted from the ensemble of $^{12}C(\alpha,\alpha)^{12}C$ spectra at variable incident energy [24–26] like those shown in Fig. 2. One can see that a homogenous distribution of C is observed, indicating the formation of uniform films.

Figure 3a, b shows the C to Ti ratios as a function of methane partial pressure for two different substrate

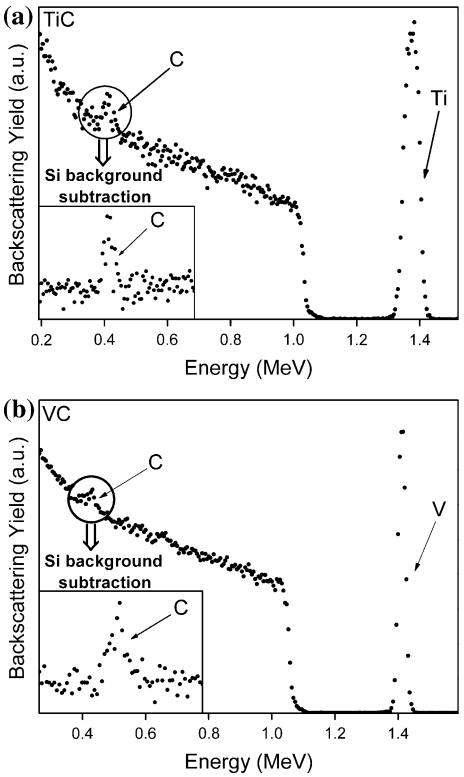


**Fig. 1** Rutherford backscattering spectra of 2 MeV $He^+$ incident particles from **a** TiC and **b** VC films deposited on Si(001)

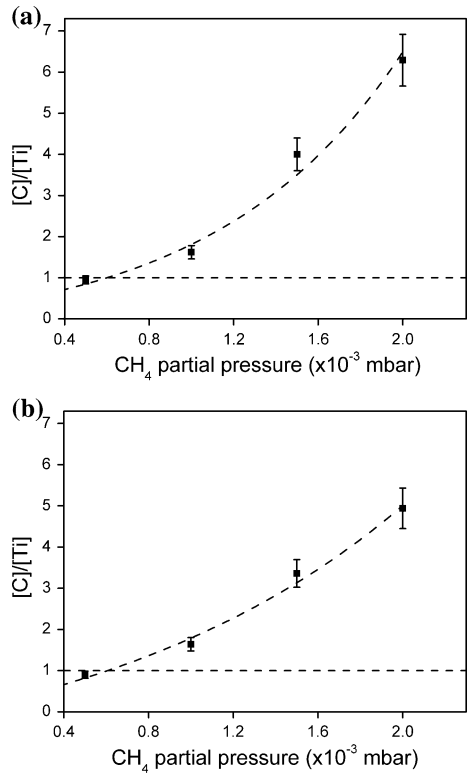


**Fig. 3** C/Ti ratio versus methane partial pressure at 50 W of target power for substrates at **a** room temperature (20 °C) and **b** 420 °C. *Line* is only to guide the eyes

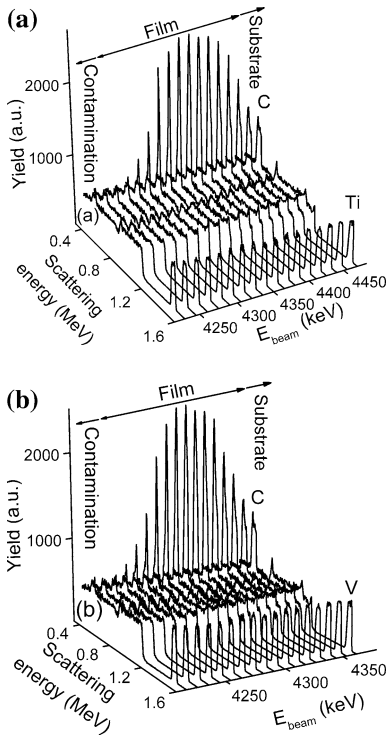


**Fig. 2** Yield of the $^{12}C(\alpha,\alpha)^{12}C$ nuclear resonant scattering near the resonance energy of 4.26 MeV from **a** TiC and **b** VC films on Si deposited at a substrate temperature of 450 °C

temperatures, 20 and 420 °C, as determined by RBS and resonant scattering analyses. For both substrate temperatures, stoichiometric film, C/Ti = V/C = 1 are obtained for a $CH_4$ partial pressure of $0.5 \times 10^{-3}$ mbar. Thus, the present results establish also favorable substrate temperature and $CH_4$ pressure to deposit TiC/VC multilayers aiming at superhard coatings.

Figure 4a shows the C to Ti concentration ratio as a function of substrate temperature during deposition. Figure 4 shows that at 400 °C, the C/Ti and C/V ratios are close to one, indicating ideal $CH_4$ pressure and substrate temperature to deposit TiC/VC multilayers. It is worth recalling here that, since the stoichiometric film presents high hardness [3, 10], deposition conditions leading to stoichiometric films is an important issue for any practical application. However, the same is not necessarily true for friction and wear characteristics, although the $H^3/E^2$ parameter points out and the results in the literature mentioned above point out in this direction.

## Deposition rates

Figure 5a, b show the TiC and VC film thicknesses as a function of deposition time, at substrate temperature of 400 °C and $CH_4$ partial pressure of $0.5 \times 10^{-3}$ mbar, for

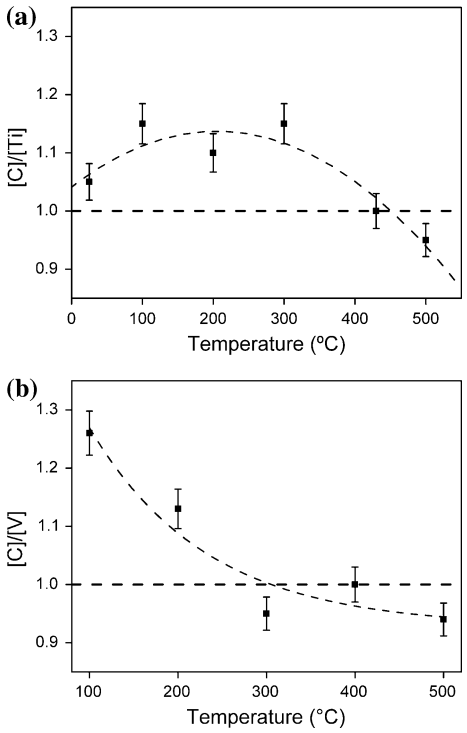


**Fig. 4** C/Ti and C/V ratio versus substrate temperature at 50 W: **a** Ti/C and **b** V/C films. Both samples deposited at $0.5 \times 10^{-3}$ mbar of $CH_4$. *Line* is only to guide the eyes

two different DC powers, namely 50 and 100 W. The film thicknesses were calculated based on the experimentally determined Ti, V, and C areal densities and the densities of TiC and VC obtained by X-ray reflectometry analysis, as described below. This leads to the following relations:

$$10^{15}\ \mathrm{Ti\,cm^{-2}} = 0.176\ \mathrm{nm}, \quad (1)$$

$$10^{15}\ \mathrm{V\,cm^{-2}} = 0.137\ \mathrm{nm}. \quad (2)$$

In Table 1, the figures for the deposition rates of TiC and VC films are given for 50 and 100 W DC target power, respectively, as obtained from the linear fit of the data of Fig. 5.

## Crystallographic structure and phases

Figure 6a shows GAXRD from TiC coatings deposited at different temperatures. One can see that the increase of the substrate temperature leads to an increase of the intensity of the fcc TiC (111) and (200) diffraction peaks with respect to the intensity of the Ti (110) peak. The progressive TiC phase formation with temperature is associated with the thermally activated surface mobility of the carbon and titanium atoms.

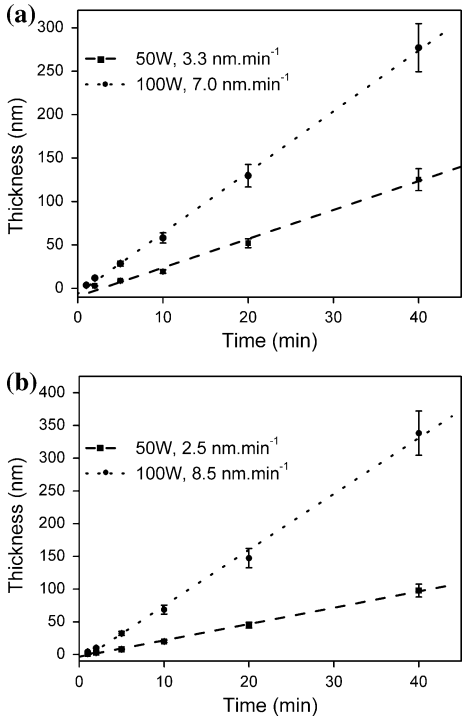


**Fig. 5** Film thickness versus deposition time for 50 and 100 W of target power, at a $CH_4$ partial pressure of $0.5 \times 10^{-3}$ mbar and substrate temperature of 400 °C for **a** TiC and **b** VC

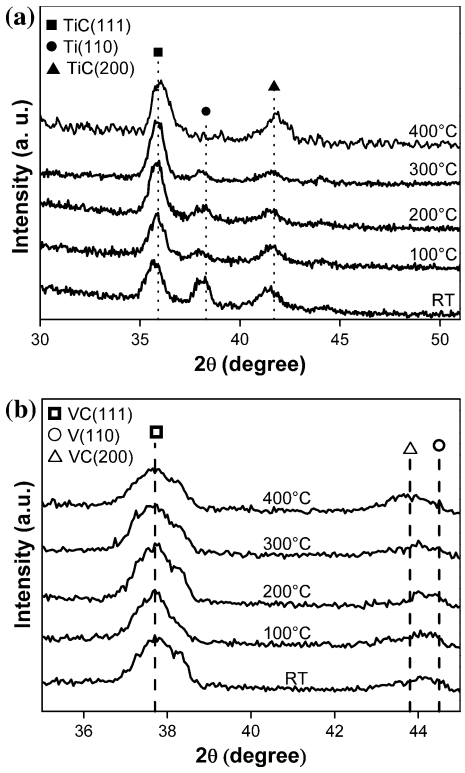


**Fig. 6** Diffractograms in $\theta \times 2\theta$ geometry from **a** TiC and **b** VC films on Si(001) at different substrate temperatures. The methane partial pressure is $0.5 \times 10^{-3}$ mbar

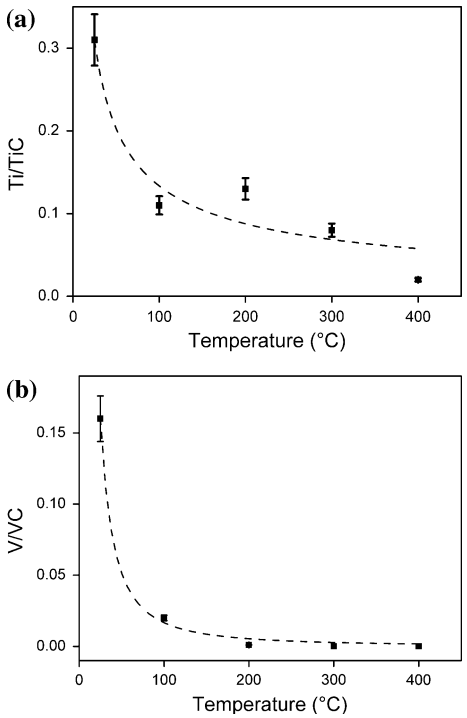


**Fig. 7** Metal to compound ratios in thin films at different substrate temperatures in **a** TiC and **b** VC films. *Line* is only to guide the eyes

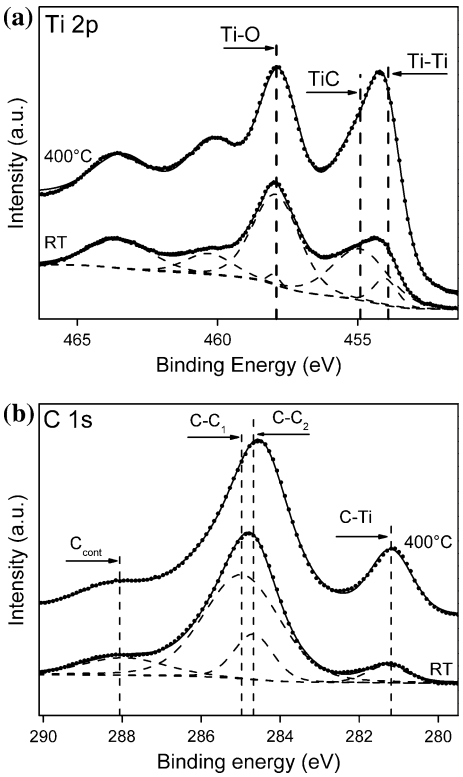


**Fig. 8** **a** Ti *2p* and **b** C *1s* X-ray photoelectron regions from TiC thin films on Si

Figure 6b shows GAXRD from VC coatings deposited at different substrate temperatures. The same picture as in TiC is observed, namely the intensities of the VC (111) and (200) diffraction peaks increase with respect to the V (110) peak as the substrate temperature increases.

Figure 7a, b show the Ti/TiC and V/VC ratios as obtained by simulations of the experimental diffractograms with the PowderCell® code [27]. Notice that for substrate temperatures above 200 °C, the metallic V phase is no longer observed, while for TiC in Fig. 7a this only happens above 300 °C.

## Chemical bonding

The chemical bonds of Ti, V, and C in the films were accessed by XPS. Figure 8a shows the Ti *2p* photoelectron regions from TiC films for substrate temperatures of 20 and 400 °C. Three different doublets, corresponding to three different bond states for Ti are observed, Ti in TiC [28], Ti in $TiO_2$ [29], and Ti in metallic Ti [30]. Since the inspection depth of XPS is about 10 nm, the presence of titanium oxide in this near-surface region of the films is expected, owing to the affinity of titanium for oxygen, similarly to TiN films after exposure to air [31]. For 400 °C substrate temperature, the TiC/$TiO_2$ spectral area ratio is much larger than for 20 °C and the intensity of metallic Ti decreases. This is consistent with the GAXRD results presented above, where the proportion of the TiC phase was seen to increase with the increasing of the substrate temperature. In Fig. 8b, C *1s* photoelectron regions for TiC films are shown. The components C–$C_1$ and C–$C_2$ at binding energies (BE) of 284.9 and 284.1 eV are assigned to amorphous carbons (a-C) phases [32–34]. The $C_{Cont}$ (289.5 eV) is assigned to hydrocarbons at the sample surface, while the peak at BE 281.5 eV is assigned to TiC. Here again, the proportion between the spectral area of the component assigned to C in TiC films with respect to the other components is larger for 400 °C substrate temperature than for 20 °C. Thus, the XPS results confirm the facts observed by GAXRD, namely that the formation of the TiC stoichiometric compound is favored at the higher substrate temperatures.

V *2p* and C *1s* photoelectron regions from VC films on Si [35] are shown in Fig. 9, confirming the general trends discussed in the last paragraph for TiC, including the presence of $V_2O_5$ in the near-surface region of the films. The formation of VC and the increase of its proportion with respect to the other spectral components as the substrate temperature increases are also observed here.

## Film densities and thicknesses

The results of XRR for TiC and VC films on Si, deposited with the substrates at 400 °C, are shown in Fig. 10.

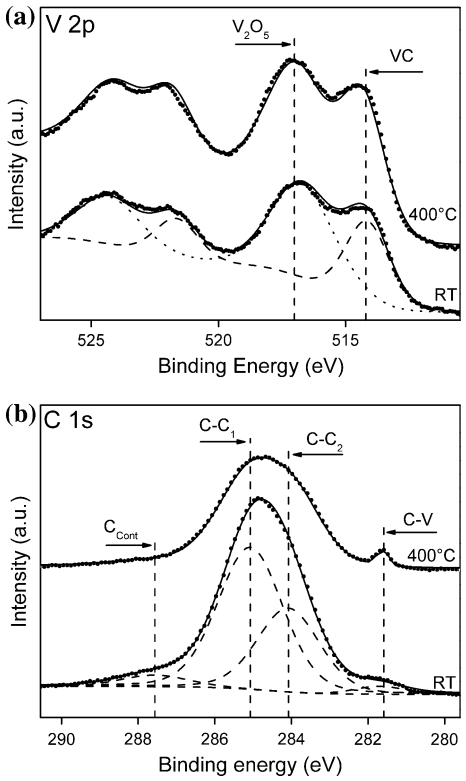


**Fig. 9** **a** V *2p* and **b** C *1s* X-ray photoelectron regions from VC thin films on Si

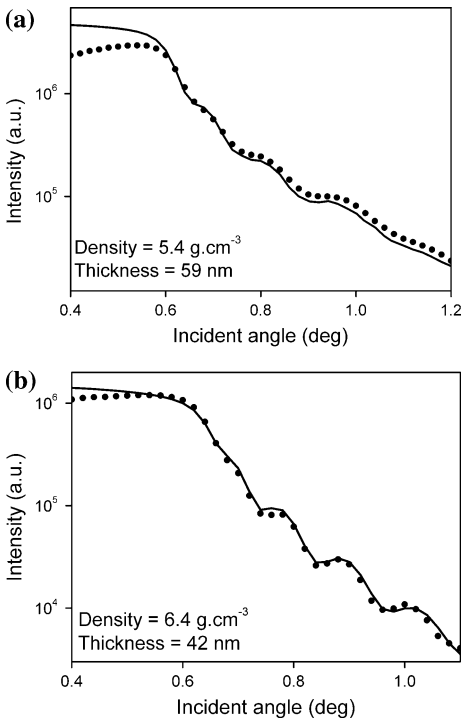


**Fig. 10** X-ray reflectometry for **a** TiC and **b** VC thin films at 50 W and 400 °C. *Dots* are the experimental data and *solid lines* are the simulations

Simulations of the XRR data [36] allowed the determination of the film thicknesses and densities, whose figures are given in Fig. 10. The densities of the films as determined by XRR are seen to be somehow higher than those for the bulk materials [37]. This fact was used in the present work as a correction in the thicknesses determined by RBS and, consequently, as a correction in the deposition rates.

## Correlations with hardness and tribological performance

The search described above for optimal conditions of deposition of stoichiometric, crystalline TiC, and VC films is a critical issue for practical applications, since previous studies demonstrated that hardness, friction, and wear behavior of these materials can be strongly influenced by these physicochemical and structural characteristics [1, 3, 10, 20, 21]. The deposition rate to stoichiometric films is also an issue of practical interest concerning processing costs. Thus, C/Ti or C/V ratios of 1, no C segregation in the films, crystalline structures, and moderate oxide layers in near-surface regions seem to be essential for good protective action of the coatings. In the present work, $CH_4$ partial pressures around $0.5 \times 10^{-3}$ mbar, substrate temperatures around 400 °C, seem to be optimal to reach the compositional and structural targets mentioned in the previous paragraph. Under these conditions, typical deposition rates may be 10 nm $min^{-1}$ or more, according to the target power.

We have measured the hardness and elastic modulus for VC and TiC films for depositions in $0.5 \times 10^{-3}$ mbar of $CH_4$, as a function of substrate temperature. The results for VC films, together with the extracted $H^3/E^2$ are given in Fig. 11. A hardness of 35 GPa as determined here for VC is comparable to the best results found in the literature. The data for TiC (not shown) indicate a similar behavior. Thus, the hardness and elastic moduli determined here point out to a maximum $H^3/E^2$, and therefore a good resistance to wear, for stoichiometric, crystalline carbide films. Some mechanical properties like hardness, modulus of elasticity, and $H^3/E^2$ for carbides films from the literature are given in Table 2. Another criterion has been used to predict the wear behavior of carbide coatings, namely the combination of hardness and fracture toughness [38, 39]. Although this last criterion is also valid, we did not addressed it in the present work since it is much less used.

Furthermore, the wear resistance of stoichiometric VC and TiC films deposited on AISI H12 steel were also approached, using pin-on-disc tests. A large reduction (of about a factor of 40) on volumetric wear with respect to the uncoated steel were observed, confirming the previsions of the $H^3/E^2$ criterion. On the other hand, the experimentally determined densities of the films here produced indicate

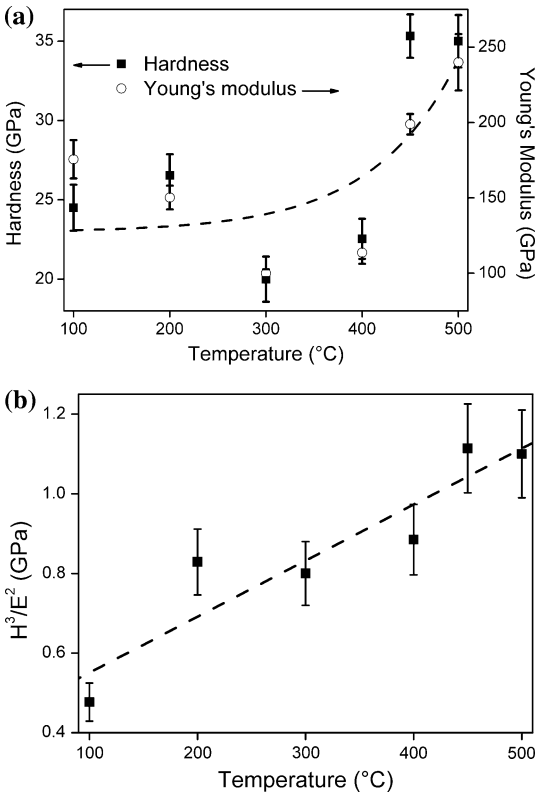


**Fig. 11** **a** Hardness and Young modulus and **b** $H^3/E^2$ ratios versus substrate temperature for VC films deposited on Si(001). *Line* is only to guide the eyes

**Table 2** Mechanical properties of carbides from references [1, 7, 11]

| Carbide | $H$ (GPa) | $E$ (GPa) | $H^3/E^2$ (GPa) |
|---|---|---|---|
| TiC | 28–35 | 300–500 | 0.1–0.4 |
| VC | 20–30 | 268–430 | 0.1–0.4 |
| TaC | 16–24 | 241–722 | 0.05–0.2 |

values slightly above the bulk values. This fact should certainly contribute also to hardness and wear resistance.

## Conclusions

The dependence of the physiochemical and structural characteristics of DC reactive sputtered deposited TiC and VC films on the reactive gas ($CH_4$) partial pressure and on the substrate temperature were investigated here. Elementary C/Ti and C/V concentration ratios of 1 were reached for $CH_4$ partial pressures around $0.5 \times 10^{-3}$ mbar and substrate temperatures around 400 °C.

The phases composing the films include TiC, Ti, and C excess, as well as $TiO_2$ in near-surface regions of the TiC films. On the other hand, VC, V, and C, together with $V_2O_5$ in near-surface regions, are identified in the VC films. The increase of substrate temperature leads to a decrease of the concentration of metallic Ti or V, with respect to TiC or VC compounds. Metallic Ti or V eventually vanishes from the films by increasing the substrate temperatures during deposition, whereas C excess disappears for $CH_4$ partial pressures below $0.5 \times 10^{-3}$ mbar.

The film densities determined here are slightly higher than the bulk densities of the corresponding materials, whereas the deposition rates are compatible with current requirements for commercial production.

The experimental $H^3/E^2$ figures indicate a pronounced wear resistance increase as the films become stoichiometric and crystalline, while preliminary wear tests of TiC and VC coatings of tool steel in the conditions described here confirm this picture. In conclusion, we can say that stoichiometric, crystalline, and very dense films can produce excellent protective VC and TiC coatings concerning wear resistance.

**Acknowledgements** The authors would like to acknowledge CNPq, Capes, Fapergs for financial support.

## References

1. Lee S, El-bjeirami O, Perry SS, Didziulis SV, Frantz P, Radhakrishnan G (2000) J Vac Sci Technol B 18:69
2. Wang GB (1997) Wear 212:25
3. Fang T-H, Jian S-R, Chuu D-S (2004) Appl Surf Sci 228:365
4. Prengel HG, Pfouts WR, Santhanam AT (1998) Surf Coat Technol 102:183
5. Singh J, Wolfe DE (2005) J Mater Sci 40:1. doi:10.1007/s10853-005-5682-5
6. Brama M, Rhodes N, Hunt J, Ricci A, Teghil R, Migliaccio S, Rocca CD, Leccisotti S, Lioi A, Scandurra M, De Maria G, Ferro D, Pu F, Panzini G, Politi L, Scandurra R (2007) Biomaterials 28:595
7. Subramanian C, Strafford KN, Wilks TP, Ward LP (1996) J Mater Process Technol 56:385
8. Hou X, Liu X, Guo M, Chou K-C (2008) J Mater Sci 43:6193. doi:10.1007/s10853-008-2928-z
9. Shimada S, Mochidsuki K (2004) J Mater Sci 39:581. doi:10.1023/B:JMSC.0000011514.46932.e2
10. Galvan D, Pei YT, Hosson JThM (2006) Surf Coat Technol 201:590
11. Recco AAC, Oliveira IC, Massi M, Maciel HS, Tschiptschin AP (2007) Surf Coat Technol 202:1078
12. Soldán J, Musil J (2006) Vacuum 81:531
13. Yang S, Chang Y, Lin D, Wang D, Wu W (2008) Surf Coat Technol 202:2176
14. Choy KL (2003) Prog Mater Sci 48:57
15. Tang J, Zabinski JS, Bulman JE (1997) Surf Coat Technol 91:69
16. Quinto DT (1996) Int J Refract Met Hard Mater 14:7
17. Rist O, Murray PT (1991) Mater Lett 10:323
18. Helmersson U, Lattemann M, Bohlmark J, Ehiasarian AP, Gudmundsson JT (2006) Thin Solid Films 513:1
19. Portolan E, Amorim CLG, Soares GV, Aguzzoli C, Perottoni CA, Baumvol IJR, Figueroa CA (2009) Thin Solid Films 517:6493
20. Shao N, Feng L, Mei F, Li G (2004) J Mater Sci 39:5533. doi:10.1023/B:JMSC.0000039280.50013.91

21. Pancielejko M, Precht W, Czyzniewski A (1999) Vacuum 53:57
22. Chu WK, Mayer JW, Nicolet MA (1978) Backscattering spectrometry. Academic Press, New York
23. Feldman LC, Mayer JW, Picraux ST (1982) Materials analysis by ion channeling. Academic Press, New York
24. Driemeier C, Baumvol IJR (2008) Nucl Instrum Methods Phys Res B 266:2041
25. Östling M, Petersson CS, Possnert G (1983) Nucl Instrum Methods 218:439
26. Jones CM, Phillips GC, Harris RW, Beckner EH (1962) Nucl Phys 37:1
27. Kraus W, Nolze G (2000) PowderCell for Windows Version 2.4
28. Frantz P, Didziulis SV (1998) Surf Sci 412/413:384
29. Guillot J, Chappé JM, Heintz O, Martin N, Imhoff L, Takadoum J (2006) Acta Mater 54:3067
30. Guemmaz M, Mosser A, Parlebas J-C (2000) J Electron Spectrosc Relat Phenom 107:91
31. Aguzzoli C, Tentardini EK, Figueroa CA, Kwietniewski C, Miotti L, Baumvol IJR (2009) Appl Phys A Mater Sci Process 94:263
32. Lewin E, Persson POÅ, Lattemann M, Stüber M, Gorgoi M, Sandell A, Ziebert C, Schäfers F, Braun W, Halbritter J, Ulrich S, Eberhardt W, Hultman L, Siegbahn H, Svensson S, Jansson U (2008) Surf Coat Technol 202:3563
33. Lin J, Moore JJ, Mishra B, Pinkas M, Sproul WD (2008) Thin Solid Films 517:1131
34. Hu Y, Li L, Cai X, Chen Q, Chu PK (2007) Diamond Relat Mater 16:181
35. Choi J-G (1999) Appl Surf Sci 148:64
36. Colombi P, Agnihotri DK, Asadchikov VE, Bontempi E, Bowen DK, Chang CH, Depero LE, Farnworth M, Fujimoto T, Gibaud A, Jergel M, Krumrey M, Lafford TA, Lamperti A, Ma T, Matyi RJ, Meduna M, Milita S, Sakurai K, Shabel'nikov L, Ulyanenkov A, Van der Lees A, Wiemert C (2008) J Appl Crystallogr 41:143
37. Shackelford JF, Alexander W (2001) Materials science and engineering handbook. CRC Press, LLC, Boca Raton
38. Ding J, Meng Y, Wen S (2000) Thin Solid Films 371:178
39. Casellas D, Caro J, Molas S, Prado JM, Valls I (2007) Acta Mater 55:4277